

Tribological Performance Studies of Waterborne Polyurethane Coatings with Aligned Modified Graphene Oxide@Fe₃O₄

Tao Bai,* Zhou Liu, Zeguang Pei, Wenqi Fang, and Yuan Ma



Cite This: *ACS Omega* 2021, 6, 9243–9253



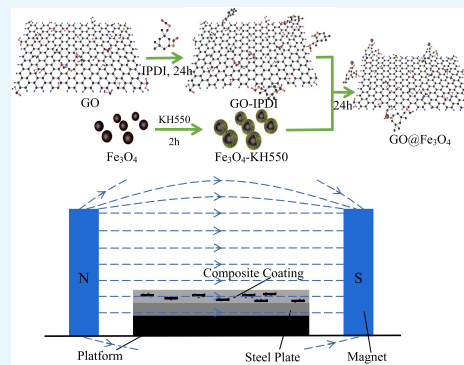
Read Online

ACCESS |

Metrics & More

Article Recommendations

ABSTRACT: In this study, the chemical graft method was used to connect modified graphene oxide (GO) and Fe₃O₄ through covalent bonds. To make full use of the tribological properties of graphene, aligned graphene oxide@Fe₃O₄/waterborne polyurethane (GO@Fe₃O₄/WPU) was prepared in a magnetic field and tribological experiments were carried out on it. The GO@Fe₃O₄ was characterized by Fourier transform infrared (FTIR) spectroscopy, X-ray diffraction (XRD), X-ray photoelectron spectroscopy (XPS), and a transmission electron microscopy (TEM). The characterization results show that Fe₃O₄ is successfully loaded on the surface of GO and GO@Fe₃O₄ has better dispersibility in WPU. Among the coatings without alignment inducement of GO@Fe₃O₄, 0.5 wt % GO@Fe₃O₄/WPU has the lowest friction coefficient and wear rate. In addition, the 0.5 wt % aligned GO@Fe₃O₄/WPU composite coating has the lowest friction coefficient and wear rate compared with nonaligned and pure WPU coatings. The excellent tribological properties of the aligned composite coating come from its ability to quickly form a uniform and continuous transfer film on the friction counterpart, which avoids direct friction between the friction counterpart and the coating.



1. INTRODUCTION

In the process of automobile manufacturing, the stamping and forming of the side peripheral panels and the door inner panels have to undergo a series of complex deformations, such as bending and reverse bending.¹ Due to the high friction between the steel plate and the mold and the low hardness of the galvanized layer, serious friction problems will cause scrapping of the parts.^{2,3} Coating with a lubricating coating on the sheet material can effectively improve its friction problems.^{4–6} Among various polymers, WPU has a wide range of applications in the friction field because of its excellent mechanical properties, easy modification, environmental protection, and no pollution.^{7–9} However, pure WPU cannot meet the requirements of antifriction and wear resistance under high-strength conditions. The tribological properties of the polymer can be improved by adding lubricants such as molybdenum disulfide,^{10,11} graphite,¹² and polytetrafluoroethylene.¹³

With its extremely low coefficient of friction, atomic smooth surface, and low interlayer shear resistance, graphene has attracted considerable attention of many scholars in the field of lubrication,^{14–16} especially as a nanoadditive to improve the tribological properties of polymers.^{17,18} Since graphene is extremely easy to agglomerate and difficult to disperse in most solvents, surface modification of graphene by chemical modification is crucial to improve the dispersion and stability of graphene in the polymer matrix.^{19–21} Mo et al. used KH550 to modify GO to obtain functionalized GO (FGO) with good

dispersibility and compatibility in the polyurethane matrix. The results showed that the friction and corrosion resistance of the composite coating with 0.25–0.5% FGO are the best.²²

Graphene is a two-dimensional sheet material with anisotropy; its distribution in the polymer matrix will affect its excellent performance in composite materials.^{23,24} Dai et al. used the coprecipitation method to modify Fe₃O₄ on the reduced graphene oxide (RGO) and realized the aligned FRGO/WPU composite material by the magnetic field induction method. The aligned FRGO/WPU composites showed excellent performance, and the dielectric loss is significantly higher than nonaligned FRGO/WPU composites.²⁵ Liu et al. synthesized reduced graphene oxide-Fe₃O₄@polyphosphazene/bismaleimide (RGO-Fe₃O₄@PZM/BMI) nanocomposites to improve the mechanical and tribological properties of BMI composites. In their study, the elastic strength and impact strength of composites containing 0.4 and 0.8 wt % RGO-Fe₃O₄@PZM increased by 31.3 and 54.5% compared with pure BMI. After adding 0.8 wt % RGO-Fe₃O₄@PZM, the wear rate of the coating dropped from 13.5

Received: February 5, 2021

Accepted: March 17, 2021

Published: March 26, 2021



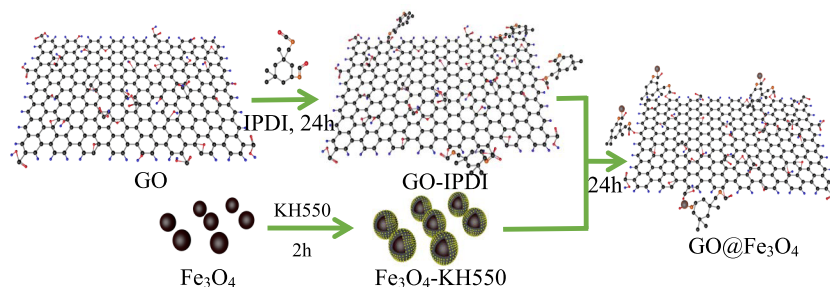


Figure 1. Schematic illustration for the preparation of GO@Fe₃O₄ composites.

$\times 10^{-6}$ to 1.0×10^{-6} mm³/(N·m) and the frictional coefficient of the coatings reduced by three times at the same time.²⁶ To the best of our knowledge, studies have been reported on graphene and its composite coatings, which mainly focused on the research on the additive components of the coating, and the other properties of the composite coating, the ultrathin sheet structure, and excellent self-lubricating performance of graphene inspired us to study performance improvement brought by its aligned distribution.

To our knowledge, there are few studies that applied oriented GO@Fe₃O₄ to WPU coatings to improve the tribological properties. First, the Fe₃O₄ particles were loaded on GO through the covalent reaction of the amino groups in the modified Fe₃O₄ and the isocyanate groups in the GO (Figure 1).^{27–29} Then, the GO@Fe₃O₄ with different mass fractions were added to the WPU, and the GO@Fe₃O₄ were aligned in the coating by a magnetic-field-induced method (Figure 2). The tribological performances of the aligned and

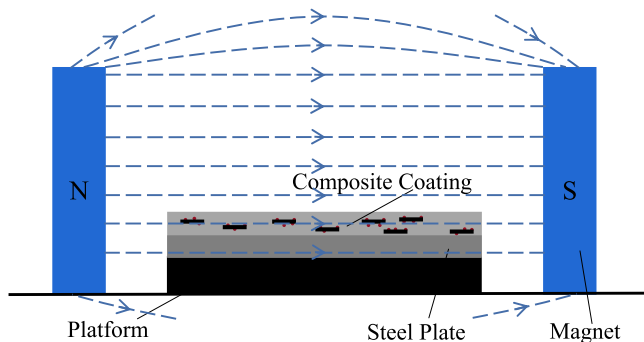


Figure 2. Schematic diagram of the coating cured in a magnetic field.

the nonaligned GO@Fe₃O₄ composite coating were investigated. Finally, the friction and wear mechanism of the GO@Fe₃O₄/WPU composite coating was studied and discussed.

2. RESULTS AND DISCUSSION

2.1. Characterization of GO@Fe₃O₄. The FTIR spectra of Fe₃O₄, Fe₃O₄-KH550, and GO@Fe₃O₄ are shown in Figure 3. For Fe₃O₄, the Fe–O bond at 590 cm⁻¹ is the characteristic absorption peak of Fe₃O₄.³⁰ In the Fe₃O₄-KH550 spectrum, the absorption peak at 569 cm⁻¹ is attributed to the Fe–O bond stretching vibration, and the strong absorption peak near 1083 cm⁻¹ is the stretching vibration of the Si–O–Si bond, indicating that Fe₃O₄ nanoparticles are modified with the silane molecules.³¹ For the GO@Fe₃O₄ spectrum, the absorption peak at 569 cm⁻¹ is assigned to the Fe–O bond, the peak near 1632 cm⁻¹ is attributed to the stretching vibration of the skeleton carbon ring C=C and the C=O in

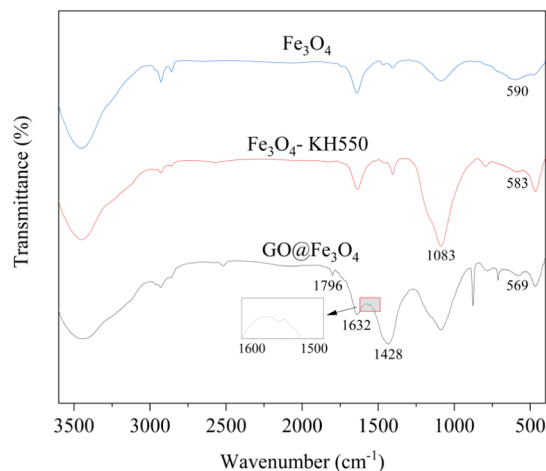


Figure 3. FTIR spectra of Fe₃O₄, Fe₃O₄-KH550, and GO@Fe₃O₄.

the carbonyl functional group at 1796 cm⁻¹, and the peaks at 1632 and 1796 cm⁻¹ are characteristic peaks of GO, indicating the presence of GO and Fe₃O₄ nanoparticles in the composite.³² The N–H bending vibration of the secondary amide appears at 1550 cm⁻¹, indicating that GO and Fe₃O₄ are successfully grafted through chemical bonds.³³

To study the changes of the GO inner structure before and after modification, GO, Fe₃O₄, and GO@Fe₃O₄ were characterized by XRD. As shown in Figure 4, there is a strong peak of GO around $2\theta = 10.82^\circ$, which is the diffraction peak of GO on the (001) plane.³⁴ The intensity of the diffraction peak of the (001) crystal plane of GO@Fe₃O₄ is significantly weaker than GO, and the diffraction peak shifts to the left from

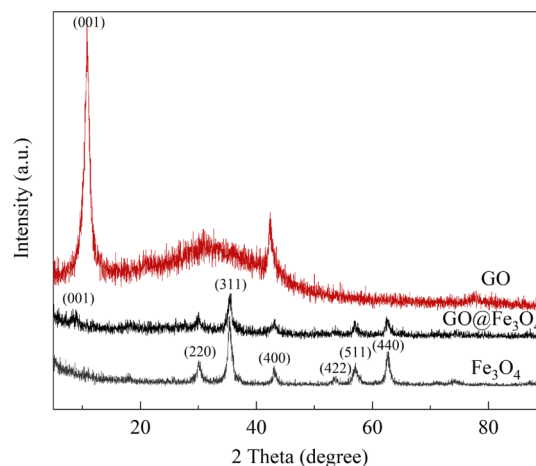


Figure 4. XRD spectra of GO, Fe₃O₄, and GO@Fe₃O₄.

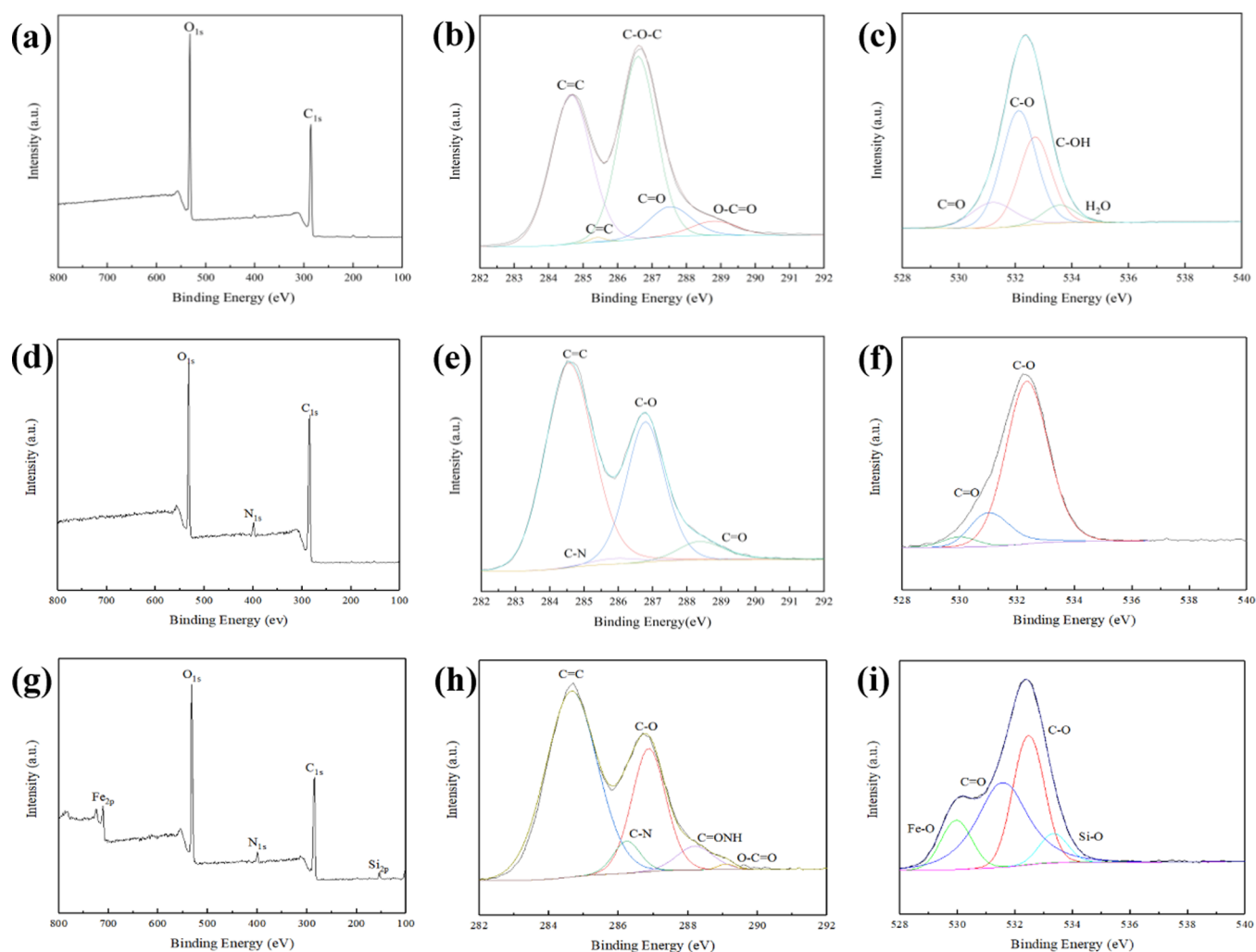


Figure 5. XPS survey scan spectra of GO (a), GO-IPDI (d), and GO@Fe₃O₄ (g); C 1s high-resolution XPS spectra of GO (b), GO-IPDI (e), and GO@Fe₃O₄ (h); O 1s high-resolution XPS spectra of GO (c), GO-IPDI (f), and GO@Fe₃O₄ (i).

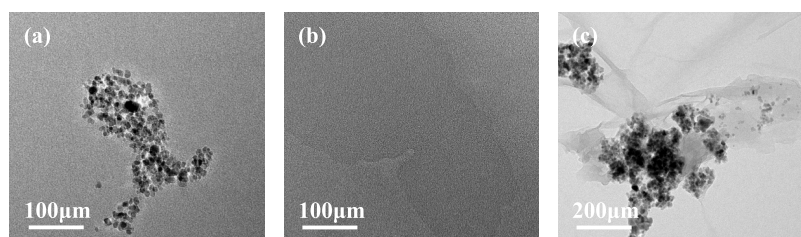


Figure 6. TEM images of Fe₃O₄ (a), GO (b), and GO@Fe₃O₄ (c).

$2\theta = 10.82^\circ$ ($d = 8.1699 \text{ \AA}$) to $2\theta = 8.41^\circ$ ($d = 10.5050 \text{ \AA}$) after Fe₃O₄ is loaded on GO, indicating that the interlayer distance expanded.³⁵ In addition to the diffraction peaks of GO, the diffraction peaks appearing at $2\theta = 30.1, 35.4, 43.1, 53.4, 57.1, 62.6,$ and 73.9° are highly consistent with the cubic spinel crystal structure of Fe₃O₄ (JCPDS Card No. 19-0629).

The formation of covalent bonds between GO and Fe₃O₄ was also confirmed by XPS, as shown in Figure 5. Figure 5b,c shows the C 1s and O 1s high-resolution XPS spectra of GO, respectively; Figure 5e,f shows the C 1s and O 1s high-resolution XPS spectra of GO-IPDI, respectively; and Figure 5h,i shows the C 1s and O 1s high-resolution XPS spectra of GO@Fe₃O₄, respectively. As can be seen from Figure 5b, the peaks at 284.6, 286.6, and 287.4 eV were assigned to C=C,

C–O, and C=O bonds of GO, respectively.^{36,37} An obvious N 1s peak appears in Figure 5d compared with Figure 5a, which represents that nitrogen-containing functional groups have been introduced on the GO surface.³⁸ It is observed from Figure 5e that 284.6, 286.8, and 288.4 eV correspond to C=C, C–O, and C=O, respectively. Moreover, a new peak appears at 286.2, which is a C–N covalent bond, indicating that IPDI has a surface modification effect on GO.^{39,40} Fe 2p and Si 2p peaks appear in Figure 5g, indicating that Fe₃O₄ is introduced on the surface of GO. In Figure 5h, it is observed that 284.8, 286.3, 287.2, 288.2, and 289.1 eV correspond to C=C, C–N, C–O, O=CNH, and O–C=O, respectively. In Figure 5i, 530.0, 531.5, 532.5, and 533.3 eV correspond to Fe–O, C=O,

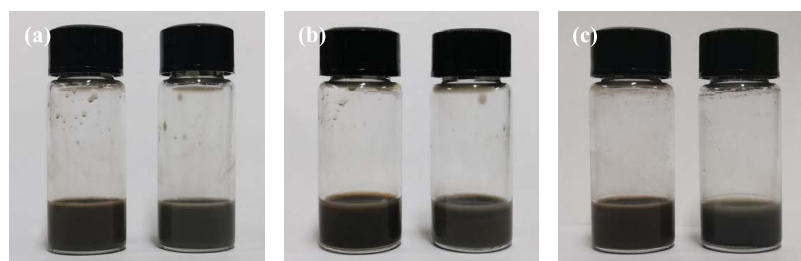


Figure 7. Dispersion degree images of GO@Fe₃O₄ (left) and GO (right), (a) after dispersion, (b) after standing for 1 h, and (c) after standing for 4 h.

C–O, and Si–O, respectively.⁴¹ The results show that Fe₃O₄ is successfully grafted to GO.

The micromorphologies of GO, Fe₃O₄, and GO@Fe₃O₄ were studied by TEM. As shown in Figure 6c, a large amount of Fe₃O₄ nanoparticles with a relatively uniform size is supported on the GO surface. Based on the above characterization, Fe₃O₄ is successfully grafted to GO.

The dispersibilities of 0.5 wt % GO and GO@Fe₃O₄ in WPU are shown in Figure 7. Two solutions are in good dispersion after ultrasonic dispersion for 1 h. The 0.5 wt % GO/WPU starts to precipitate after 1 h of static and completely precipitates after 4 h, while the 0.5 wt % GO@Fe₃O₄/WPU has good dispersibility, indicating that the dispersion of modified GO in WPU becomes better.

2.2. Characterization of the GO@Fe₃O₄/WPU Composite. To further study the interface interaction between GO@Fe₃O₄ and WPU, the cross sections of pure WPU and its composite were investigated by SEM. As shown in Figure 8a,

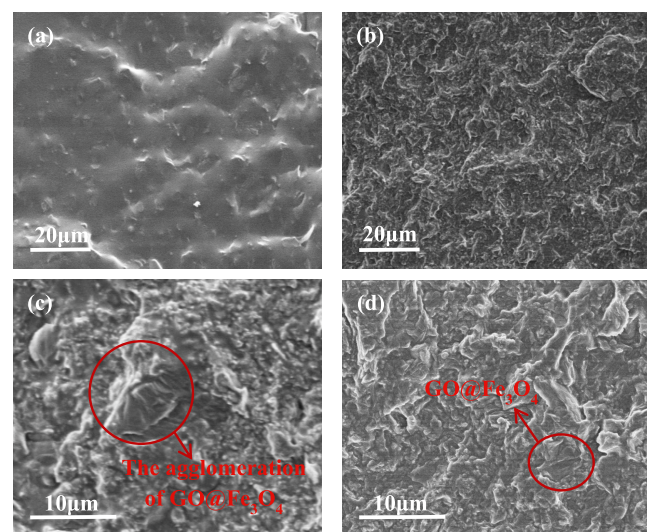


Figure 8. SEM images of cross sections of WPU composites with and without GO@Fe₃O₄ additives, (a) pure WPU, (b) aligned GO@Fe₃O₄/WPU composite, (c) composite with 2.0% addition, and (d) composite with 0.5% addition.

when GO@Fe₃O₄ is not added to WPU, the cross section is relatively smooth and the cracks extend like a river, which is a characteristic of brittle fracture. When GO@Fe₃O₄ is added to WPU (Figure 8b–d), due to the introduction of a large number of interfaces and the compatibility of GO@Fe₃O₄ with WPU being better, the cross section of the composites becomes rougher. Compared with the cross section of pure WPU, the cross sections of GO@Fe₃O₄/WPU composites

show a stronger interaction. Figure 8b is the fracture of the aligned composite. It can be seen that GO@Fe₃O₄ with an uneven and protruding cross section is covered by resin and embedded in the WPU, which is due to the uniform distribution of GO@Fe₃O₄ in the WPU and the good interface interaction between the Fe₃O₄ and WPU. The even dispersion of GO@Fe₃O₄ in WPU can promote GO to give full play to its excellent lubricating properties. The good interface interaction between GO@Fe₃O₄ and WPU can improve the mechanical properties of the composite coating, thus probably inhibiting the growth of microcracks in the friction process and contributing to enhancing the wear resistance of the composite coating. The agglomeration caused by excessive GO@Fe₃O₄ in the resin can be clearly seen in Figure 8c, which indicates that the interfacial interaction between the GO@Fe₃O₄ and WPU is weak. Hence, agglomeration may cause GO@Fe₃O₄ to peel off easily during the friction process, accordingly affecting the wear resistance of the coating. Nevertheless, when the added amount of GO@Fe₃O₄ is 0.5 wt %, its dispersion in the WPU is uniform, as shown in Figure 8d. However, the aligned arrangement of GO@Fe₃O₄ in WPU cannot be clearly seen in the sectional diagram of the aligned GO@Fe₃O₄/WPU composite. It may be due to the good interfacial interaction between the GO@Fe₃O₄ and the WPU. Further, the amount of GO@Fe₃O₄ added to the WPU is small, so the filler is covered with a large amount of resin.

2.3. Tribological Performance of the Nonaligned GO@Fe₃O₄/WPU Composite Coatings. Tribological experiments were carried out on nonaligned composite coatings with GO@Fe₃O₄ mass fractions of 0, 0.3, 0.5, 1, and 2 wt %. The effects of GO@Fe₃O₄ on the antifriction and wear resistance of WPU coatings are discussed. As shown in Figure 9, the friction coefficient of pure WPU is relatively high and fluctuates greatly, with an average friction coefficient of 0.8. With an increase of the GO@Fe₃O₄ content, the friction coefficient shows a gradual decrease trend, the friction coefficient curve also tends to be stable, and the fluctuation decreases. The average friction coefficient reaches the minimum at 0.5 wt %, which is 0.45. When the mass fraction gradually increases to 2 wt %, the friction coefficient of the GO@Fe₃O₄/WPU composite coating also increases, and the average friction coefficient reaches 0.72. Moreover, it is still lower than that of the pure WPU coating. Compared with the pure WPU coating and the coating with the added GO@Fe₃O₄ amount of 2 wt %, the tribological performance of the coating with the GO@Fe₃O₄ content not exceeding 1 wt % is more stable. This is due to the good lubricating effect of GO@Fe₃O₄ and the uniform dispersion in the resin. During the friction process, the relative sliding between graphenes enhances its excellent lubrication performance. At the same time, Fe₃O₄ nanoparticles with a

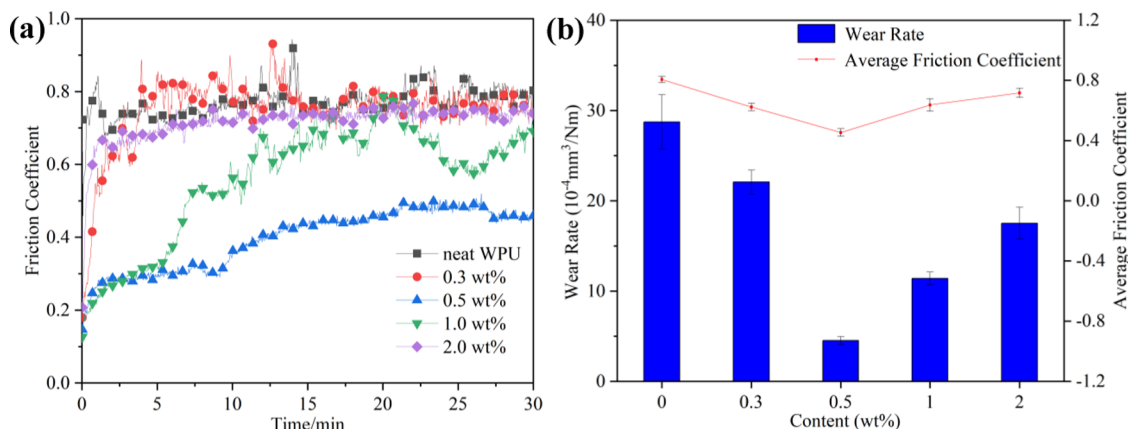


Figure 9. Tribological performance of the GO@Fe₃O₄/WPU composite coatings, (a) real-time friction coefficient and (b) average friction coefficient and wear rate.

spherical structure load on the surface of the graphene act as rolling bearings, which can convert sliding friction into rolling friction. In addition, a part of GO@Fe₃O₄ will adhere to the friction counterpart to form a transfer lubricating film, so GO@Fe₃O₄ has a certain antifriction performance. When the content of GO@Fe₃O₄ in WPU is high, GO@Fe₃O₄ will agglomerate seriously. The agglomeration seriously affects the interfacial bonding force between GO@Fe₃O₄ and WPU, which leads to the easy exfoliation of fillers from the WPU during the friction process so that its antifriction performance cannot be fully exerted.

The wear rate of the GO@Fe₃O₄/WPU composite coatings is displayed in Figure 9. With the increase of the GO@Fe₃O₄ content, the wear rate of the composite coating shows a trend of decrease first and then increase. In Figure 9b, the wear rate of the pure WPU coating is the largest, reaching 26.67×10^{-4} mm³/(N·m). With the increase of the GO@Fe₃O₄ content, the wear rate of the composite coating gradually decreases; when the mass fraction is 0.5 wt %, the coating wear rate is the smallest, 4.48×10^{-4} mm³/(N·m); when the added amount exceeds 0.5 wt %, the wear rate of the composite coating gradually increases, reaching 17.49×10^{-4} mm³/(N·m) at 2 wt %. From the cross-sectional morphology of the coating in Figure 10, it can be seen that the composite with 0.5 wt %

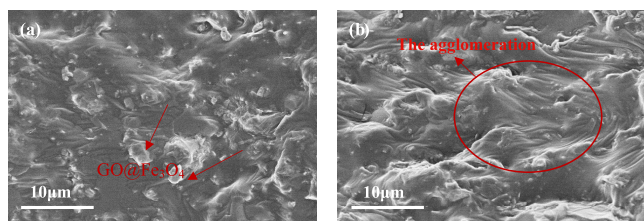


Figure 10. SEM images of the cross-sectional morphology of the GO@Fe₃O₄/WPU coatings, (a) 0.5 wt % GO@Fe₃O₄ and (b) 2 wt % GO@Fe₃O₄.

GO@Fe₃O₄ has better filler dispersion than the composite with 2 wt % GO@Fe₃O₄. The addition of GO@Fe₃O₄ to the WPU can deflect the crack growth path and hinder the rapid propagation of microcracks in the coating, thereby preventing the formation of wear debris during the wear process and reducing the wear rate of the coating.⁴² However, excess GO@Fe₃O₄ will form agglomeration in the resin, which makes the crack expand more easily. The agglomeration will cause the

coating to peel off during friction and then affect the wear resistance of the coating.

2.4. Tribological Performance of the Aligned GO@Fe₃O₄/WPU Composite Coatings. The friction coefficient and wear rate of the aligned GO@Fe₃O₄/WPU composite coating were tested, and the effect of GO@Fe₃O₄ alignment on the tribological performance of the composite coating was studied. Figure 11a indicates the influence of the GO@Fe₃O₄ content on the antifriction performance of the aligned composite coating. With the increase of the GO@Fe₃O₄ content, the average friction coefficients of aligned and nonaligned GO@Fe₃O₄/WPU coatings both decrease first and then increase. Aligned and nonaligned GO@Fe₃O₄/WPU coatings have the minimum average friction coefficient at 0.5 wt %, which are 0.45 and 0.25, respectively. When the mass fraction gradually increases to 2 wt %, the friction coefficient of the aligned GO@Fe₃O₄/WPU composite coating also increases, and the average friction coefficient reaches 0.4. Comparing Figures 9 and 11, it can be clearly seen that the friction coefficient of the aligned composite coating is significantly lower than that of the pure WPU coating and the nonaligned GO@Fe₃O₄ coating. The average friction coefficient decreases from 0.8 to 0.25, indicating that the aligned distribution of GO@Fe₃O₄ can significantly improve the antifriction performance of WPU coating. Since the isocyanate functional group grafted on the modified GO surface reacts with the carbamate group in the WPU, it enhances the binding force between the matrix and filler. Therefore, a lot of energy can be absorbed during the friction process to prevent the growth of microcracks. Comparing Figure 9a with Figure 11a, it can be seen that the average friction coefficient of the aligned GO@Fe₃O₄/WPU coating (0.25) is lower than that of the nonaligned coating (0.45). The distribution of GO@Fe₃O₄ in the nonaligned composite coating is shown in Figure 15a. In the nonaligned composite coating, since GO@Fe₃O₄ presents a random morphology in the WPU, the shear force required to transfer GO@Fe₃O₄ from the coating to the friction counterpart is different during the friction process. The shearing force required for GO@Fe₃O₄ in the vertical direction is greater than for GO@Fe₃O₄ distributed in the horizontal direction, so an uneven and discontinuous transfer film may be formed, which limits the excellent antifriction performance of GO. By aligning the GO@Fe₃O₄ with a magnetic field, it can fully exert its antifriction effect, thereby improving the antifriction perform-

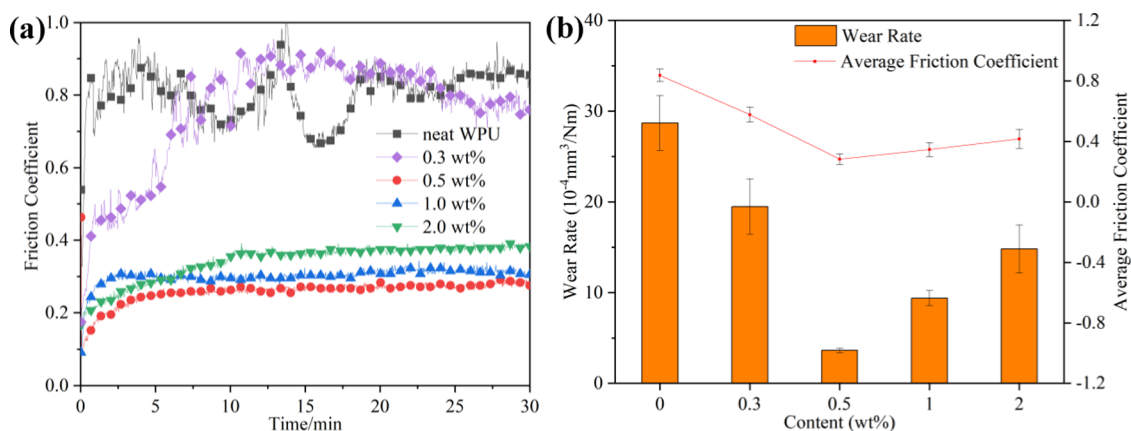


Figure 11. Friction coefficients of aligned GO@Fe₃O₄/WPU composite coatings: (a) real-time friction coefficient and (b) average friction coefficient and wear rate.

ance of the composite coating. During friction, the friction counterpart first acts on the resin part of the GO@Fe₃O₄/WPU coating. Then, the friction pair slides on the resin embedded with aligned GO@Fe₃O₄. Due to the aligned distribution of GO@Fe₃O₄ in the resin matrix, the shear force required for the exfoliation of GO during friction is smaller, which can reduce the friction resistance. In addition, the performance of each part of the coating is relatively average, so a uniform and continuous transfer film is formed easily on the surface of the friction pair during the friction process, which significantly reduces the friction coefficient of the GO@Fe₃O₄/WPU composite coating. When the GO@Fe₃O₄ content exceeds 0.5 wt %, the average friction coefficient of the composite coating begins to rise, but it is still lower than that of the pure WPU coating. This phenomenon is due to the agglomeration of GO@Fe₃O₄ in the matrix.⁴³ The agglomeration is easy to peel from the WPU, which will greatly affect the formation of an effective transfer film on the surface of the friction counterpart. In addition, it will cause more microcracks during the friction process, thus reducing the bearing capacity of the composite coating during the friction process and affecting the excellent antifriction performance of GO@Fe₃O₄ itself.

The wear rates of pure WPU coating and aligned GO@Fe₃O₄/WPU composite coating are shown in Figure 11b. Comparing Figure 9b with Figure 11b, it can be seen that the wear rate of the aligned GO@Fe₃O₄/WPU composite coating is lower than that of the nonaligned coating and the wear rate of the pure WPU coating is the largest, up to $26.67 \times 10^{-4} \text{ mm}^3/(\text{N}\cdot\text{m})$. The wear rate decreases with the increase of the GO@Fe₃O₄ content. The wear rate of the 0.5 wt % GO@Fe₃O₄/WPU coating is the smallest, which is $3.60 \times 10^{-4} \text{ mm}^3/(\text{N}\cdot\text{m})$. As a result of the aligned and uniform distribution of GO@Fe₃O₄ in the resin, the stress during friction is evenly distributed and delays the formation of crack sources. It also can expand the crack propagation path and delay the role of wear debris, thereby improving the wear resistance of the coating. When the content of GO@Fe₃O₄ reaches 2 wt %, the wear rate increases to $14.81 \times 10^{-4} \text{ mm}^3/(\text{N}\cdot\text{m})$. This indicates that the GO@Fe₃O₄ agglomerate seriously causes the microcracks in the coating to grow more easily. The wear mechanism of GO@Fe₃O₄/WPU will be discussed in the next section.

2.5. Wear Mechanisms of the Aligned GO@Fe₃O₄/WPU Composite Coatings. It can be seen from the above

experimental results that adding GO@Fe₃O₄ to the coating can significantly improve the antifriction and wear resistance of the WPU coating. Figure 12 shows the SEM images of the surface

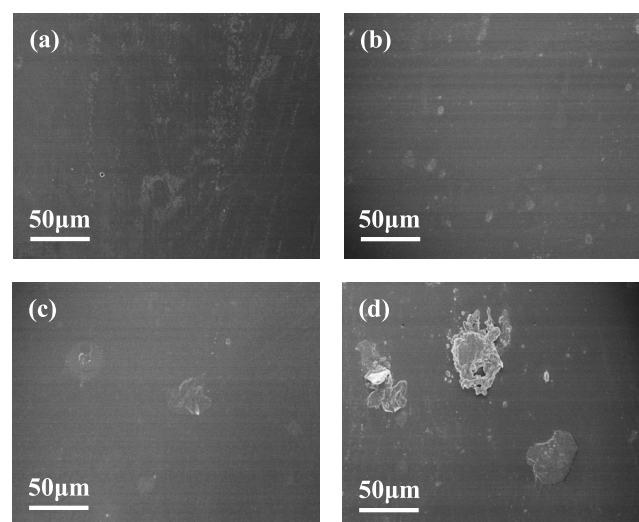


Figure 12. SEM images of the surface morphology taken from the aligned GO@Fe₃O₄/WPU composite coating: (a) 0.3 wt % GO@Fe₃O₄ content, (b) 0.5 wt % GO@Fe₃O₄ content, (c) 1 wt % GO@Fe₃O₄ content, and (d) 2 wt % GO@Fe₃O₄ content.

morphology of the composite coating with different GO@Fe₃O₄ contents. It can be seen that when the added amounts of GO@Fe₃O₄ are 0.3, 0.5, and 1 wt %, the dispersibility of the filler in the resin is better and there is no agglomeration phenomenon. The isocyanate groups on the surface of GO@Fe₃O₄ can covalently bond with the carbamate groups in WPU, which greatly improves the dispersibility of GO@Fe₃O₄ and its interfacial bonding force with the WPU.⁴⁴ When the amount of GO@Fe₃O₄ added reaches 2 wt %, the surface of the coating is rougher and a large number of agglomerates can be observed. When the amount of GO@Fe₃O₄ is higher, the nanomaterials tend to agglomerate in the resin to reduce the surface free energy. The coating is subjected to reciprocating friction pressure during the friction process. Due to the weak interfacial bonding, microcracks are prone to generate and propagate between GO@Fe₃O₄ and WPU. These microcracks are generated under the surface of the coating and are usually difficult to observe on the surface of the coating. When these

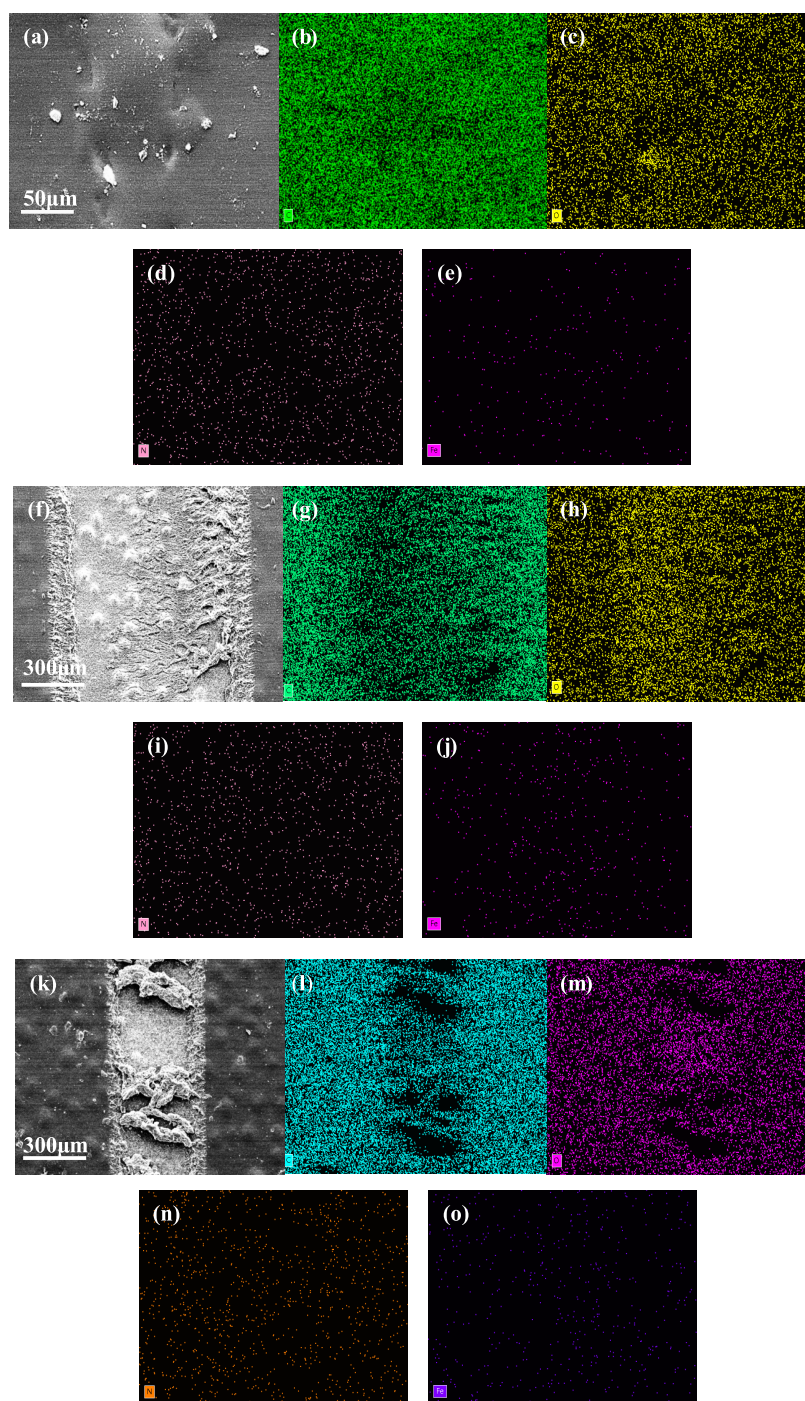


Figure 13. SEM images of the worn surface and corresponding elemental mapping images taken from the aligned GO@Fe₃O₄/WPU composite coating: (a) 0.5 wt % GO@Fe₃O₄ content; (b–e) C, N, O, and Fe element distribution of 0.5 wt % GO@Fe₃O₄ content; (f) 1 wt % GO@Fe₃O₄ content; (g–j) C, N, O, and Fe element distribution of 1 wt % GO@Fe₃O₄ content; (k) 2 wt % GO@Fe₃O₄ content; and (l–o) C, N, O, and Fe element distribution of 2 wt % GO@Fe₃O₄ content.

internal microcracks continue to propagate and eventually connect with the coating surface, the wear debris may be peeled from the coating, thus affecting the wear rate of the coating.

The overall morphology of the coating worn surface and its corresponding elemental mapping image are observed in Figure 13. Figure 13a,f,k are SEM images of worn surfaces of the GO@Fe₃O₄/WPU coatings with 0.5, 1, and 2 wt %, respectively. Figure 13b–e,g–j,l–o shows the C, O, N, and Fe element mapping images on the worn surfaces of 0.5, 1, and 2

wt % coatings. From Figure 13, when the GO@Fe₃O₄ addition values are 0.5, 1, and 2 wt %, the surface of the coatings is worn to varying degrees; the 2 wt % coating surface wear is the most serious. Due to the high concentration of filler added to the WPU, agglomeration will occur in the coating, leading to easy exfoliation of the coating and the appearance of large pieces of debris during the friction process.²⁴ Besides, the elemental mapping image of the worn surface of the 2 wt % GO@Fe₃O₄/WPU coating shows that there were several places where the element distribution was blank, indicating that the coating on

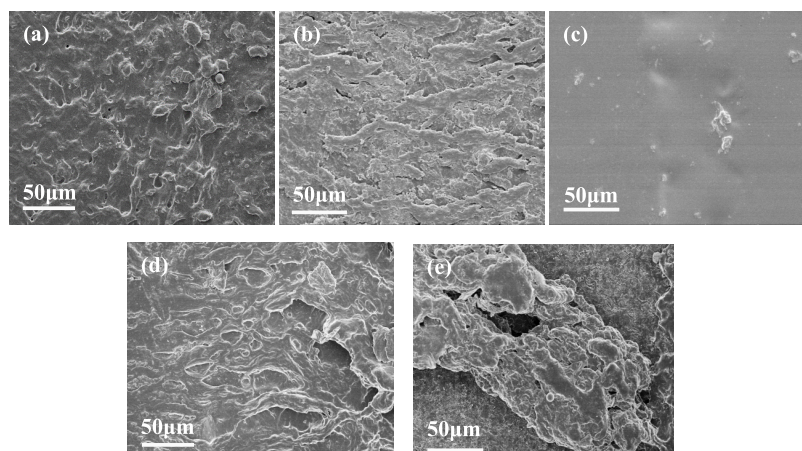


Figure 14. SEM images of the worn surface taken from aligned GO@Fe₃O₄/WPU composite coatings with GO@Fe₃O₄ contents of (a) 0 wt %, (b) 0.3 wt %, (c) 0.5 wt %, (d) 1 wt %, and (e) 2 wt %.

the surface of the steel plate is completely exfoliated. The result corresponds to the high wear rate shown in Figure 12b. However, the worn surface of the 0.5 wt % GO@Fe₃O₄/WPU coating was smooth, as seen from the SEM images. It can be observed from the elemental mapping images that the distribution of various elements in the coating is relatively uniform, with only a small amount of coating peeling, and its wear rate is the lowest. It may be transferred to the friction counterpart during the friction process, and a thin transfer film is formed on it.

The SEM images of the wear surface of aligned GO@Fe₃O₄/WPU composite coatings with different GO@Fe₃O₄ contents are further observed, as shown in Figure 14. Figure 14a shows the worn surface morphology of a pure WPU coating; adhesive wear occurs on the coating. The wear surface is rough and there is a lot of wear debris distribution, which indicates that microcracks are generated and spread inside the coating during the friction process. This phenomenon corresponds to the high wear rate of the coating shown in Figure 11b. Comparing Figure 14a–d, it can be seen that with the weight fraction of GO@Fe₃O₄ increasing, the amount of wear debris distributed on the wear surface is significantly reduced. It can be observed from Figure 14c that the wear surface of the 0.5 wt % GO@Fe₃O₄/WPU composite coating is the smoothest and has no obvious wear debris, which shows the best wear resistance. Due to the covalent attachment between the isocyanate group on the surface of GO@Fe₃O₄ and the aminomethyl ester in the WPU, good compatibility and interfacial interaction between the filler and the WPU matrix are achieved. When the microcracks inside the coating spread to the vicinity of the well-dispersed GO@Fe₃O₄, the aligned GO@Fe₃O₄ in the resin matrix will extend the crack path, absorb more energy, and prevent further expansion of microcracks; meanwhile, Fe₃O₄ nanoparticles loaded on the GO can fill the worn part of the coating surface, so the wear resistance of the composite coating is improved. Compared with the nonaligned composite coating, the friction shearing force of the separation between the GO layers in the aligned composite coating is smaller and the aligned GO@Fe₃O₄ in the resin matrix can be transferred to the friction counterpart faster. So it can quickly form a uniform transfer film on the surface of the friction pair during the friction process,^{23,45} which slows down the shearing effect of the metal pair on the composite coating and ultimately improves the wear resistance

of the composite coating. Moreover, as shown in Figure 14e, when the amount of GO@Fe₃O₄ is 2 wt %, it can be seen that the wear surface of the coating is very rough and accompanied by wear debris. This may be attributed to the agglomerate in the 2 wt % GO@Fe₃O₄/WPU, so its ability to prevent microcrack propagation is drastically reduced.⁴⁶ The agglomerated GO@Fe₃O₄ may hinder the formation of a continuous transfer film, resulting in increased wear debris on the wear surface.

Based on the above experimental data and conclusions, the mechanism model of wear behavior of the GO@Fe₃O₄/WPU composite coating is obtained as shown in Figure 15. Figure 15a shows the nonaligned composite coating with GO@Fe₃O₄ added. Figure 15b is the friction mechanism of the coating. When the microcracks expand to the vicinity of well-dispersed and aligned GO@Fe₃O₄ under the action of friction, GO@Fe₃O₄ will deflect and extend the crack path due to the good interfacial bonding force between GO@Fe₃O₄ and WPU. Moreover, the energy of crack growth is absorbed by GO@Fe₃O₄, and the growth of microcracks is hindered. Nonaligned coatings also have a certain wear resistance. Figure 15c represents the aligned composite coating with GO@Fe₃O₄. The figure shows that GO@Fe₃O₄ is uniformly dispersed in the composite coating. By magnetic field induction, GO@Fe₃O₄ is aligned. As shown in Figure 15d, the aligned distribution of GO@Fe₃O₄ in the coating can make the stress on the coating smaller and evenly dispersed. It slows down the formation of microcracks, thereby reducing the generation of wear debris and ultimately improving the wear resistance of the coating. Moreover, when the aligned distribution of GO@Fe₃O₄ is subjected to friction, the frictional shear force for separation between the GO is smaller and the performance of each part of the coating surface is more even. It is easier to quickly form a uniform transfer film on the friction counterpart, which can also reduce the friction coefficient of the composite coating.

3. CONCLUSIONS

In this work, surface modification of GO and Fe₃O₄ was carried out by chemical grafting, and Fe₃O₄ was successfully loaded on the GO. Then, different concentrations of GO@Fe₃O₄ are added to the WPU and cured in a magnetic field to obtain aligned GO@Fe₃O₄/WPU composite coating. The tribological experiment results show that after adding GO@

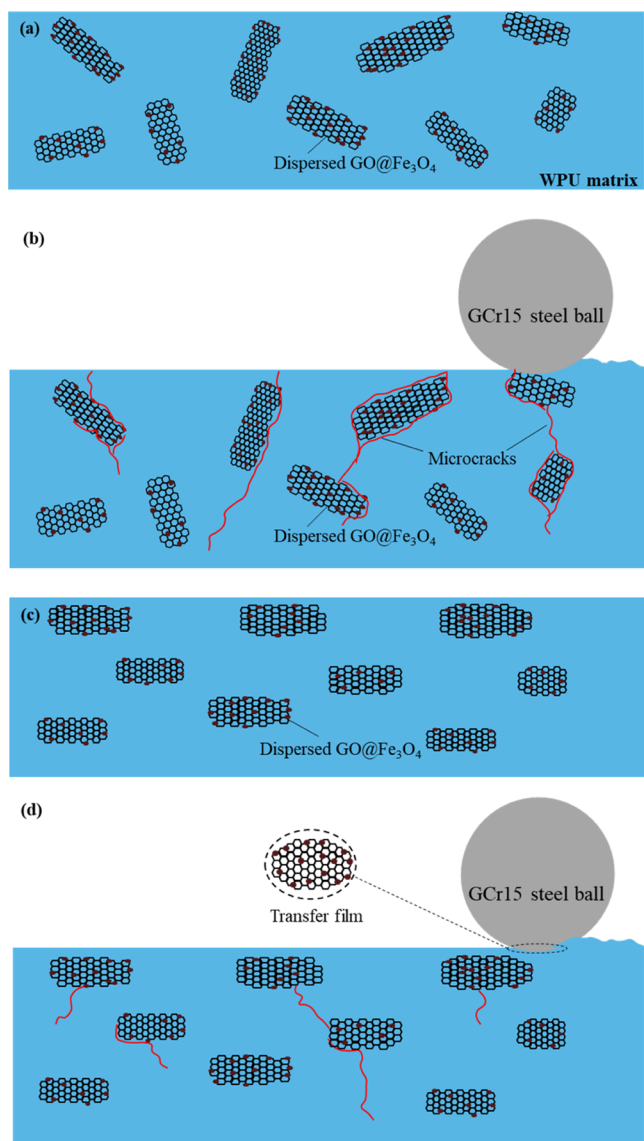


Figure 15. Mechanism scheme for the wear behavior of nonaligned composite coating (a, b) and GO@Fe₃O₄/WPU aligned composite coating (c, d).

Fe₃O₄, the friction coefficient and wear rate of the composite coating are significantly decreased. The results lead to the following five conclusions.

- (1) The successful modification of GO-IPDI and Fe₃O₄-KH550 and the Fe₃O₄ successful loading on GO surfaces are confirmed by FTIR, XRD, XPS, and TEM characterization analyses.
- (2) GO@Fe₃O₄ has a certain antifriction performance, and the optimal mass fraction in the composite coating is 0.5 wt %. The wear rate and friction coefficient of the composite coating are reduced to 0.25 and $3.60 \times 10^{-4} \text{ mm}^3/(\text{N}\cdot\text{m})$, respectively.
- (3) The addition of aligned GO@Fe₃O₄ can accelerate the formation of the transfer film and further improve the tribological properties of the composite coating.
- (4) The spherical Fe₃O₄ nanoparticles loaded on the surface of the GO can fill the worn parts of the friction surface and play a repairing role.

- (5) Alignment and uniform distribution can extend the crack propagation path, delay the formation of wear debris, and improve the wear resistance of the coating.

Therefore, the aligned GO@Fe₃O₄/WPU composite material has great application potential in the field of tribology.

4. EXPERIMENTAL SECTION

4.1. Materials. Iron oxide (Fe₃O₄, 20 nm, purity $\geq 99\%$), 3-aminopropyl triethoxy silane (KH550, purity $\geq 99\%$), and isophorone diisocyanate (IPDI, purity $\geq 99\%$) were purchased from Aladdin Industrial Corporation. Graphene oxide (GO, thickness: 4–8 nm; layers: 5–10; lateral dimension: 10–50 μm , purity $\geq 95\%$) was supplied by Suzhou Tanfeng Technology Co., Ltd. Dichloromethane (purity $\geq 99.5\%$), *N,N*-dimethylformamide (DMF, purity $\geq 99.5\%$), and other chemicals were provided by Sinopharm Chemical Reagent Co., Ltd. Waterborne polyurethane (WPU) was obtained from Anhui Huatai New Material Co., Ltd.

4.2. Preparation of GO@Fe₃O₄. The preparation process of GO@Fe₃O₄ is shown in Figure 1. First, 0.2 g of GO was dispersed in 20 mL of DMF, and 1.78 g of IPDI was added into a three-necked flask under a nitrogen atmosphere with stirring for 24 h. The solution was washed 3–4 times with dichloromethane and then dried out in an oven at 80 °C for 12 h before the next modification. Second, 0.1 g of Fe₃O₄ was dispersed in 21.6 mL of anhydrous ethanol by ultrasonication for 30 min, and then 12 mL of KH550 was added slowly into the suspension by mechanical stirring for 2 h. The resulting Fe₃O₄-KH550 was washed with anhydrous ethanol 3 times, followed by drying at 80 °C for 12 h.⁴⁷ Finally, 0.08 g of GO-IPDI was dispersed in 25 mL of DMF by ultrasonication for 30 min. Later, 0.08 g of Fe₃O₄-KH550 was added into the suspension by mechanical stirring for 24 h. Then, the solution was washed 3–4 times with dichloromethane and GO@Fe₃O₄ powder was obtained by drying in an oven at 80 °C for 12 h.

4.3. Fabrication of Aligned GO@Fe₃O₄/WPU Composite Coatings. To study the influence of GO@Fe₃O₄ on the tribological properties of WPU coatings, composite coatings with 0, 0.3, 0.5, 1, and 2 wt % GO@Fe₃O₄ were prepared. After that, the effect of alignment distribution of GO@Fe₃O₄ on tribological properties of WPU coatings will be analyzed. Figure 2 shows a schematic diagram of the magnetic-field-aligned distribution of GO@Fe₃O₄. For preparing the aligned GO@Fe₃O₄/WPU composite coating, the coating was cured in a magnetic field environment.

The galvanized steel plate was selected as the matrix material. The galvanized steel was sanded with 800-mesh sandpaper and then underwent absolute ethanol ultrasonic treatment to remove the dirt on the surface of the steel sheet before coating. To prepare the aligned GO@Fe₃O₄/WPU coating, GO@Fe₃O₄ with different mass fractions were added to 6 g of WPU and further GO@Fe₃O₄ and WPU were mixed thoroughly by the ball-milling method. Next, the processed steel sheet was brushed with a wire bar coater of 70 μm coating thickness to obtain the GO@Fe₃O₄/WPU coating, and the coating was placed in a 0.5 T magnetic field at 60 °C for 1 h to obtain the aligned GO@Fe₃O₄/WPU coating, as shown in Figure 2. Nonaligned GO@Fe₃O₄/WPU coating was obtained without a magnetic field.

4.4. Characterization. The successful modification of Fe₃O₄ and GO and the chemical bond connection between Fe₃O₄ and GO were proved by Fourier transform infrared

spectroscopy (FTIR, Nicolet6700) and X-ray photoelectronic spectroscopy (XPS, Escalab 250Xi, China). The internal structure and defects of GO and GO@Fe₃O₄ were determined with X-ray diffraction (XRD, D/MAX-2550VB+/PC, Japan) and identified with Cu K α radiation. The microstructures and morphologies of GO, Fe₃O₄, and GO@Fe₃O₄ were characterized by transmission electron microscopy (TEM, JEM-2100F, Japan). The morphologies of the cross section, the coating surface, and the worn surface were obtained by field emission scanning electron microscopy (FESEM, SU8010, China). The elemental component information was determined by an energy-dispersive spectrometer (EDS) in the FESEM. To study the dispersibilities of GO@Fe₃O₄ and GO in WPU, 0.5 wt % GO@Fe₃O₄/WPU and GO/WPU solutions were prepared, and the dispersion degrees of GO and GO@Fe₃O₄ in WPU were compared after being allowed to stand for a certain period of time.

4.5. Tribological Test of the Composite Coatings. The tribological properties of the aligned GO@Fe₃O₄/WPU and nonaligned GO@Fe₃O₄/WPU composite coatings were tested by high-speed reciprocating friction and a wear testing tribometer (HSR-2M, Zhong Ke Kai Hua Corporation, China) under dry conditions. Tribological experiments were carried out three times for each composite coating of different mass fractions, and the average value of the three experimental results was taken as the average friction coefficient of the coating. In the test, a GCr15 bearing steel ball (diameter: 6 mm) was used as the friction counterpart, the friction load was 3 N, the running speed was 220 t/min, the reciprocating distance was 5 mm, and the friction time was 30 min.

The wear rates of the aligned and nonaligned GO@Fe₃O₄/WPU composite coatings were calculated by the formula^{48,49}

$$A = \frac{V}{S \cdot F} \quad (1)$$

where A is the wear rate of the coating (mm³/(N·m)), V is the volumetric wear measured by the HSR-2M surface wear measurement component, S represents the reciprocating distance (m), and F represents the friction load (N).

AUTHOR INFORMATION

Corresponding Author

Tao Bai – College of Mechanical Engineering, Donghua University, Shanghai 201620, China; Engineering Research Center of Advanced Textile Machinery, Ministry of Education, Shanghai 201620, China; orcid.org/0000-0002-0569-8183; Email: baitao@dhu.edu.cn

Authors

Zhou Liu – College of Mechanical Engineering, Donghua University, Shanghai 201620, China

Zeguang Pei – College of Mechanical Engineering, Donghua University, Shanghai 201620, China; Engineering Research Center of Advanced Textile Machinery, Ministry of Education, Shanghai 201620, China; orcid.org/0000-0003-3973-6528

Wenqi Fang – Baosteel Research Institute, Baoshan Iron and Steel Co., Ltd., Shanghai 201900, China

Yuan Ma – Baosteel Research Institute, Baoshan Iron and Steel Co., Ltd., Shanghai 201900, China

Complete contact information is available at:

<https://pubs.acs.org/10.1021/acsoomega.1c00688>

Notes

The authors declare no competing financial interest.

ACKNOWLEDGMENTS

This work was financially supported by the National Key Research and Development Program of China (2016YFB0302300).

REFERENCES

- (1) Li, G.; Long, X.; Liang, Z.; Yang, P.; Liu, Y. Research progress of friction and surface damage in stamping forming of galvanized advanced high strength steel sheet. *J. Plast. Eng.* **2018**, *25*, 11–20.
- (2) Wen, N.-M.; Cheng, G.-P. Properties of Baosteel inorganic-lubricant-coated galvanized steel sheet for automotive body panels. *Baosteel Tech. Res.* **2018**, *12*, 9–15.
- (3) Chen, M.-Z. Defect and Its Improvement in Galvanized Sheet Steel Painting. *Automob. Technol. Mater.* **2004**, *09*, 41–44.
- (4) Hill, D.; Holliman, P. J.; McGettrick, J.; Appelman, M.; Chatterjee, P.; Watson, T. M.; Worsley, D. Study of the tribological properties and ageing of alkyphosphonic acid films on galvanized steel. *Tribol. Int.* **2018**, *119*, 337–344.
- (5) Jo, D. H.; Noh, S.-G.; Park, J.-T.; Kang, C.-H. Improved Corrosion and Abrasion Resistance of Organic-Inorganic Composite Coated Electro-galvanized Steels for Digital TV Panels. *Corros. Sci. Technol.* **2015**, *14*, 213–217.
- (6) Carlsson, P.; Bexell, U.; Olsson, M. Friction and Wear Mechanisms of Thin Organic Permanent Coatings Deposited on Hot-Dip Coated Steel. *Wear* **2001**, *247*, 88–99.
- (7) Bai, T.; Lv, L.; Du, W.; Fang, W.; Wang, Y. Improving the Tribological and Anticorrosion Performance of Waterborne Polyurethane Coating by the Synergistic Effect between Modified Graphene Oxide and Polytetrafluoroethylene. *Nanomaterials* **2020**, *10*, 137–154.
- (8) Chai, C.-P.; Ma, Y.-F.; Li, G.-P.; Ge, Z.; Ma, S.-Y.; Luo, Y.-J. The preparation of high solid content waterborne polyurethane by special physical blending. *Prog. Org. Coat.* **2018**, *115*, 79–85.
- (9) Wen, J. G.; Geng, W.; Geng, H. Z.; Zhao, H.; Jing, L. C.; Yuan, X. T.; Tian, Y.; Wang, T.; Ning, Y. J.; Wu, L. Improvement of Corrosion Resistance of Waterborne Polyurethane Coatings by Covalent and Noncovalent Grafted Graphene Oxide Nanosheets. *ACS Omega* **2019**, *4*, 20265–20274.
- (10) Farsadi, M.; Bagheri, S.; Ismail, N. A. Nanocomposite of functionalized graphene and molybdenum disulfide as friction modifier additive for lubricant. *J. Mol. Liq.* **2017**, *244*, 304–308.
- (11) Ji, Z.; Zhang, L.; Xie, G.; Xu, W.; Guo, D.; Luo, J.; Prakash, B. Mechanical and tribological properties of nanocomposites incorporated with two-dimensional materials. *Friction* **2020**, *8*, 813–846.
- (12) Katiyar, J. K.; Sinha, S. K.; Kumar, A. Friction and wear durability study of epoxy-based polymer (SU-8) composite coatings with talc and graphite as fillers. *Wear* **2016**, *362–363*, 199–208.
- (13) Peng, S.; Zhang, L.; Xie, G.; Guo, Y.; Si, L.; Luo, J. Friction and wear behavior of PTFE coatings modified with poly (methyl methacrylate). *Composites, Part B* **2019**, *172*, 316–322.
- (14) Liu, Y.; Ge, X.; Li, J. Graphene lubrication. *Appl. Mater. Today* **2020**, *20*, No. 100662.
- (15) Srivivya, P. D.; Charoo, M. S. Nano lubrication behaviour of Graphite, h-BN and Graphene Nano Platelets for reducing friction and wear. *Mater. Today: Proc.* **2020**, DOI: [10.1016/j.matpr.2020.04.785](https://doi.org/10.1016/j.matpr.2020.04.785).
- (16) Zhang, L.; Sun, X.; Liu, X.; He, Y.; Chen, Y.; Liao, Z.; Gao, H.; Wang, S. Alkyl Titanate-Modified Graphene Oxide as Friction and Wear Reduction Additives in PAO Oil. *ACS Omega* **2021**, *6*, 3840–3846.
- (17) Zhao, B.; Bai, T. Improving the tribological performance of epoxy coatings by the synergistic effect between dehydrated ethylenediamine modified graphene and polytetrafluoroethylene. *Carbon* **2019**, *144*, 481–491.

- (18) Stankovich, S.; Dikin, D. A.; Dommett, G. H. B.; Kohlhaas, K. M.; Ruoff, R. S.; et al. Graphene-Based Composite Materials. *Nature* **2006**, *442*, 282–286.
- (19) Feng, J. Y.; Wang, X. C.; Guo, P. Y.; Wang, Y. J.; Luo, X. M. Mechanical Properties and Wear Resistance of Sulfonated Graphene/Waterborne Polyurethane Composites Prepared by In Situ Method. *Polymers* **2018**, *10*, 75–86.
- (20) Sukur, E. F.; Onal, G. Graphene nanoplatelet modified basalt/epoxy multi-scale composites with improved tribological performance. *Wear* **2020**, 460–461, No. 203481.
- (21) Cheng, J.; Chen, S.; Zhang, F.; Shen, B.; Lu, X.; Pan, J. Corrosion- and Wear-Resistant Composite Film of Graphene and Mussel Adhesive Proteins on Carbon Steel. *Corros. Sci.* **2020**, *164*, No. 108351.
- (22) Mo, M.; Zhao, W.; Chen, Z.; Yu, Q.; Zeng, Z.; Wu, X.; Xue, Q. Excellent tribological and anti-corrosion performance of polyurethane composite coatings reinforced with functionalized graphene and graphene oxide nanosheets. *RSC Adv.* **2015**, *5*, 56486–56497.
- (23) Wang, F.; Wang, H.; Mao, J. Aligned-graphene composites: a review. *J. Mater. Sci.* **2019**, *54*, 36–61.
- (24) Liu, C.; Yan, H.; Chen, Z.; Yuan, L.; Liu, T. Enhanced tribological properties of bismaleimides filled with aligned graphene nanosheets coated with Fe₃O₄ nanorods. *J. Mater. Chem. A* **2015**, *3*, 10559–10565.
- (25) Dai, M.; Zhai, Y.; Wu, L.; Zhang, Y. Magnetic aligned Fe₃O₄-reduced graphene oxide/waterborne polyurethane composites with controllable structure for high microwave absorption capacity. *Carbon* **2019**, *152*, 661–670.
- (26) Liu, C.; Yan, H.; Lv, Q.; Li, S.; Niu, S. Enhanced tribological properties of aligned reduced graphene oxide-Fe₃O₄@polyphosphazene/bismaleimides composites. *Carbon* **2016**, *102*, 145–153.
- (27) Orooji, Y.; Mortazavi-Derazkola, S.; Ghoreishi, S. M.; Amiri, M.; Salavati-Niasari, M. Mesoporous Fe₃O₄@SiO₂-hydroxyapatite nanocomposite: Green sonochemical synthesis using strawberry fruit extract as a capping agent, characterization and their application in sulfasalazine delivery and cytotoxicity. *J. Hazard. Mater.* **2020**, *400*, No. 123140.
- (28) Stankovich, S.; Piner, R. D.; Nguyen, S. T.; Ruoff, R. S. Synthesis and exfoliation of isocyanate-treated graphene oxide nanoplatelets. *Carbon* **2006**, *44*, 3342–3347.
- (29) Li, Y.; Zhou, M.; Xia, Z.; Gong, Q.; Liu, X.; Yang, Y.; Gao, Q. Facile preparation of polyaniline covalently grafted to isocyanate functionalized reduced graphene oxide nanocomposite for high performance flexible supercapacitors. *Colloids Surf., A* **2020**, *602*, No. 125172.
- (30) Wan, X.; Zhan, Y.; Long, Z.; Zeng, G.; Ren, Y.; He, Y. High-performance magnetic poly (arylene ether nitrile) nanocomposites: Co-modification of Fe₃O₄ via mussel inspired poly(dopamine) and amino functionalized silane KH550. *Appl. Surf. Sci.* **2017**, *425*, 905–914.
- (31) Liu, H.; Zhang, Y.; Zhou, Y.; Chen, Z.; Lichtfouse, E. Self-provided microbial electricity enhanced wastewater treatment using carbon felt anode coated with amino-functionalized Fe₃O₄. *J. Water Process Eng.* **2020**, *38*, No. 101649.
- (32) Ma, Y.-X.; Li, Y.-F.; Zhao, G.-H.; Yang, L.-Q.; Wang, J.-Z.; Shan, X.; Yan, X. Preparation and characterization of graphite nanosheets decorated with Fe₃O₄ nanoparticles used in the immobilization of glucoamylase. *Carbon* **2012**, *50*, 2976–2986.
- (33) Yang, J. H.; Ramaraj, B.; Yoon, K. R. Preparation and characterization of superparamagnetic graphene oxide nanohybrids anchored with Fe₃O₄ nanoparticles. *J. Alloys Compd.* **2014**, *583*, 128–133.
- (34) Lei, L.; Xia, Z.; Zhang, L.; Zhang, Y.; Zhong, L. Preparation and properties of amino-functional reduced graphene oxide/waterborne polyurethane hybrid emulsions. *Prog. Org. Coat.* **2016**, *97*, 19–27.
- (35) Zhang, P.; Gong, J.-L.; Zeng, G.-M.; Deng, C.-H.; Yang, H.-C.; Liu, H.-Y.; Huan, S.-Y. Cross-linking to prepare composite graphene oxide-framework membranes with high-flux for dyes and heavy metal ions removal. *Chem. Eng. J.* **2017**, *322*, 657–666.
- (36) Stankovich, S.; Dikin, D. A.; Piner, R. D.; Kohlhaas, K. A.; Kleinhammes, A.; Jia, Y.; Wu, Y.; Nguyen, S. B. T.; Ruoff, R. S. Synthesis of graphene-based nanosheets via chemical reduction of exfoliated graphite oxide. *Carbon* **2007**, *45*, 1558–1565.
- (37) Li, P. F.; Zhou, H.; Cheng, X. Investigation of a hydrothermal reduced graphene oxide nano coating on Ti substrate and its nanotribological behavior. *Surf. Coat. Technol.* **2014**, *254*, 298–304.
- (38) Saha, U.; Jaiswal, R.; Singh, J. P.; Goswami, T. H. Diisocyanate modified graphene oxide network structure: steric effect of diisocyanates on bimolecular cross-linking degree. *J. Nanopart. Res.* **2014**, *16*, 2404–2424.
- (39) Zhu, Y.; Xie, W.; Gao, S.; Zhang, F.; Zhang, W.; Liu, Z.; Jin, J. Single-Walled Carbon Nanotube Film Supported Nanofiltration Membrane with a Nearly 10 nm Thick Polyamide Selective Layer for High-Flux and High-Rejection Desalination. *Small* **2016**, 5034–5041.
- (40) Zhao, Z.; Guo, L.; Feng, L.; Lu, H.; Zou, X.; et al. Polydopamine functionalized graphene oxide nanocomposites reinforced the corrosion protection and adhesion properties of waterborne polyurethane coatings. *Eur. Polym. J.* **2019**, *120*, No. 109249.
- (41) Ye, Y.; Yang, D.; Zhang, D.; Chen, H.; Zhao, H.; Li, X.; Wang, L. POSS-tetraaniline modified graphene for active corrosion protection of epoxy-based organic coating. *Chem. Eng. J.* **2020**, *383*, No. 123160.
- (42) Walker, L. S.; Marotto, V. R.; Rafiee, M. A.; Koratkar, N.; Corral, E. L. Toughening in Graphene Ceramic Composites. *ACS Nano* **2011**, *5*, 3182–3190.
- (43) Li, H.; Jin, L.; Dong, J.; Liu, L.; Li, M.; Liu, Y.; Xiao, L.; Ao, Y. Tribological performance and thermal conductivity of graphene-Fe₃O₄/poly(phenol-formaldehyde resin) hybrid reinforced carbon fiber composites. *RSC Adv.* **2016**, *6*, 60200–60205.
- (44) Wang, C.; Cheng, X. Upconversion and tribological properties of β-NaYF₄:Yb,Er film synthesized on silicon substrate. *Appl. Surf. Sci.* **2016**, *371*, 391–398.
- (45) Wang, F.; Mao, J. Double layer aligned-graphene nanosheets/styrene-butadiene rubber composites: Tribological and mechanical properties. *J. Appl. Polym. Sci.* **2019**, *136*, 46939–46948.
- (46) Zhi, X.; Yan, H.; Li, S.; Niu, S.; Liu, C.; Xu, P. High toughening and low friction of novel bismaleimide composites with organic functionalized serpentine@Fe₃O₄. *J. Polym. Res.* **2017**, *24*, No. 31.
- (47) Mirzabe, G. H.; Keshtkar, A. R. Application of response surface methodology for thorium adsorption on PVA/Fe₃O₄/SiO₂/APTES nanohybrid adsorbent. *J. Ind. Eng. Chem.* **2015**, *26*, 277–285.
- (48) Yang, K.; Shi, X.; Zhai, W.; Mahmoud Ibrahim, A. M. Wear rate of a TiAl matrix composite containing 10 wt% Ag predicted using the Newton interpolation method. *RSC Adv.* **2015**, *5*, 67102–67114.
- (49) Aigbodion, V. S.; Hassan, S. B. Experimental correlations between wear rate and wear parameter of Al–Cu–Mg/bagasse ash particulate composite. *Mater. Des.* **2010**, *31*, 2177–2180.